optica

Origin of the asymmetric light emission from molecular exciton-polaritons: supplementary material

TOMÁŠ NEUMAN[1] AND JAVIER AIZPURUA[1,2,*]

[1]Centro de Física de Materiales de San Sebastián, CFM - MPC (CSIC-UPV/EHU), Paseo Manuel Lardizabal 5, 20018 Donostia-San Sebastián, Spain
[2]Donostia International Physics Center (DIPC), 20018 Donostia-San Sebastián, Spain
[*]Corresponding author: aizpurua@ehu.eus

Published 9 October 2018

This document provides supplementary information to "Origin of the asymmetric light emission from molecular exciton-polaritons," https://doi.org/10.1364/OPTICA.5.001247. It includes more details on (i) Description of the strong coupling of the cavity mode with excitons of multiple molecules and the elimination of the de-phasing reservoir in the collective case, (ii) details about the incoherent decay of the polariton states in strong coupling, (iii) description of the truncated Hilbert space used for the numerical calculations, (iv) technical aspects of the calculation of the emission and absorption spectra, (v) comparison of the emission spectra of polaritons interacting with dephasing bath characterized by different value of the effective reservoir frequency Ω_R and (vi) comparison of absorption and emission spectra of polaritons considering a variable value of g.

1. STRONG COUPLING OF THE CAVITY MODE WITH EXCITONS OF MULTIPLE MOLECULES

In the main text we present the system Hamiltonian, $H_{\rm tot}$ [Eq. (7) of the main text], containing the molecules interacting with their local dephasing reservoirs and the cavity mode, together with the laser pumping $H_{\rm pump}$. Here we show how the Hamiltonian can be transformed into the polariton picture. We first introduce the picture of collective excitations of the molecules. To that end we introduce a new set of operators $S_i = \sum_\alpha c_{i\alpha}\sigma_\alpha$, where $c_{i\alpha}$ are coefficients that are elements of a unitary matrix such that $(c_{i1}, c_{i2}, \ldots, c_{iN})$ form a set of N orthonormal vectors. It is convenient to make the choice

$$(c_{11}, c_{12}, \ldots, c_{1N}) = \frac{1}{\sqrt{\sum_\alpha |g_\alpha|^2}}(g_1, g_2, \ldots, g_N) \tag{S1}$$

and the remaining vectors orthonormal to the first vector. With this choice S_1 becomes fully coupled to the plasmonic cavity via a new effective coupling constant $g_{\rm eff} = \sqrt{\sum_\alpha |g_\alpha|^2}$. In the following we consider that all coefficients $g_\alpha = g$ are equal ($c_{1\alpha} = 1/\sqrt{N}$) and recover the result $g_{\rm eff} = \sqrt{N}g$. We further consider the low-excitation limit where the new operators S_i become approximately bosonic and independent

$$[S_i, S_j^\dagger] \approx \delta_{ij}, \tag{S2}$$

with the transformation rules

$$\sum_\alpha \sigma_\alpha^\dagger\sigma_\alpha = \sum_i S_i^\dagger S_i, \tag{S3}$$

$$\sum_\alpha \sigma_\alpha\rho\sigma_\alpha^\dagger = \sum_{ij}\left(\sum_\alpha c_{\alpha i}c_{\alpha j}\right) S_i\rho S_j^\dagger = \sum_i S_i\rho S_i^\dagger, \tag{S4}$$

where in the second line we used the orthogonality of the coefficient vectors that we assumed to be real.

The transformation rules allow rewriting the Hamiltonian as:

$$\begin{aligned} H_{\rm tot} = &\sum_i \hbar\omega_0 S_i^\dagger S_i + \hbar\omega_c a^\dagger a + g_{\rm eff}\left(S_1 a^\dagger + S_1^\dagger a\right) + \sum_\alpha \hbar\Omega_R B_\alpha^\dagger B_\alpha \\ &+ \hbar d_R\Omega_R \sum_{ij}\left[\sum_\alpha c_{\alpha i}c_{\alpha j}\left(B_\alpha + B_\alpha^\dagger\right)\right] S_i^\dagger S_j \\ &+ \hbar\mathcal{E}\left(ae^{i\omega_L t} + a^\dagger e^{-i\omega_L t}\right) \\ &+ \sum_{ij}\left(\sum_{\alpha\beta} G_{\alpha\beta}c_{\alpha i}c_{\beta j}\right) S_i^\dagger S_j + \text{H.c.}. \end{aligned} \tag{S5}$$

and the Lindblad terms

$$\sum_\alpha \mathcal{L}_{\sigma_\alpha}(\rho) = \sum_i \mathcal{L}_{S_i}(\rho), \tag{S6}$$

with $\gamma_{\sigma_i} = \gamma_{S_i} = \gamma_\sigma$ and $\mathcal{L}_{\mathcal{O}}(\rho) = \frac{\gamma_\mathcal{O}}{2}\left(2\mathcal{O}\rho\mathcal{O}^\dagger - \{\mathcal{O}^\dagger\mathcal{O}, \rho\}\right)$.

As in the case of the single molecule, we can proceed to diagonalize the Hamiltonian part involving the bright excitonic mode strongly coupled with the cavity [neglecting for now the inter-molecular coupling in the last line of Eq. (S5)]. We thus generate a new set of annihilation operators of the lower, S_-, and the upper, S_+, polaritons

$$S_+ = \cos\theta\, S_1 + \sin\theta\, a, \tag{S7}$$
$$S_- = -\sin\theta\, S_1 + \cos\theta\, a, \tag{S8}$$

with θ defined in analogy with the single-exciton case presented in the main text. In the polaritonic picture, the system Hamiltonian becomes

$$H = \hbar\omega_+ S_+^\dagger S_+ + \hbar\omega_- S_-^\dagger S_- + \sum_{i=2}^{N}\hbar\omega_0 S_i^\dagger S_i + \sum_\alpha \hbar\Omega_\mathrm{R} B_\alpha^\dagger B_\alpha \tag{S9a}$$

$$+ \hbar d_\mathrm{R}\Omega_\mathrm{R}\left[\sum_\alpha c_{\alpha 1}c_{\alpha 1}\left(B_\alpha + B_\alpha^\dagger\right)\right]$$
$$\times\left[\cos^2\theta\, S_+^\dagger S_+ + \sin^2\theta\, S_-^\dagger S_- - \sin\theta\cos\theta(S_+^\dagger S_- + S_-^\dagger S_+)\right] \tag{S9b}$$

$$+\left[\hbar\cos\theta\, d_\mathrm{R}\Omega_\mathrm{R}\sum_{i=2}^{N}\left[\sum_\alpha c_{\alpha i}c_{\alpha 1}\left(B_\alpha + B_\alpha^\dagger\right)\right] S_i^\dagger S_+ + \mathrm{H.c.}\right] \tag{S9c}$$

$$-\left[\hbar\sin\theta\, d_\mathrm{R}\Omega_\mathrm{R}\sum_{i=2}^{N}\left[\sum_\alpha c_{\alpha i}c_{\alpha 1}\left(B_\alpha + B_\alpha^\dagger\right)\right] S_i^\dagger S_- + \mathrm{H.c.}\right] \tag{S9d}$$

$$+\hbar d_\mathrm{R}\Omega_\mathrm{R}\sum_{i,j=2}^{N}\left[\sum_\alpha c_{\alpha i}c_{\alpha j}\left(B_\alpha + B_\alpha^\dagger\right)\right] S_i^\dagger S_j \tag{S9e}$$

$$+\hbar\mathcal{E}\Big(\left[\sin\theta\, S_+ + \cos\theta\, S_-\right] e^{i\omega_\mathrm{L}t}$$
$$+\left[\sin\theta\, S_+^\dagger + \cos\theta\, S_-^\dagger\right] e^{-i\omega_\mathrm{L}t}\Big) \tag{S9f}$$

$$+\left[\sum_{j=2}^{N}\left(\sum_{\alpha\beta} G_{\alpha\beta}c_{\alpha 1}c_{\beta j}\right)\left[\cos(\theta)S_+^\dagger - \sin(\theta)S_-^\dagger\right] S_j + \mathrm{H.c.}\right] \tag{S9g}$$

$$+\Bigg[\left(\sum_{\alpha\beta} G_{\alpha\beta}c_{\alpha 1}c_{\beta 1}\right)\left[\cos\theta S_+^\dagger - \sin\theta S_-^\dagger\right]$$
$$\times\left[\cos\theta S_+ - \sin\theta S_-\right]\Bigg] \tag{S9h}$$

$$+\sum_{ij=2}^{N}\left(\sum_{\alpha\beta} G_{\alpha\beta}c_{\alpha i}c_{\beta j}\right) S_i^\dagger S_j. \tag{S9i}$$

Here Eq. (S9a) represents the system of the newly arising polariton states. The coupling of the various polaritonic modes with the dephasing reservoir is given by Eq. (S9b) to Eq. (S9e). The interaction with the reservoir will lead to population transfer among $|+\rangle$, $|-\rangle$, and the dark polaritons $|\mathrm{D}_i\rangle$. Throughout this supplementary material we are going to use S_i and $S_i^\dagger$ to denote the operators $S_i = |0\rangle\langle \mathrm{D}_i|$ and $S_i^\dagger = |\mathrm{D}_i\rangle\langle 0|$ (for $i > 1$) for brevity. Notice that in the main text S_i ($S_i^\dagger$) is denoted as S_{D_i} ($S_{\mathrm{D}_i}^\dagger$). The coherent laser pumping is included in Eq. (S9f). The term in Eq. (S9g) of the transformed Hamiltonian introduces mixing of the dark states with the bright modes that leads to formation of the dark-polariton peak in the emission spectra. Equation (S9i) represents additional interactions among the dark modes that are weak for the selected parameters.

The incoherent damping of the dephasing reservoir is included via $\mathcal{L}_{B_\alpha}(\rho)$, with $\gamma_{B_\alpha} = \gamma_B$. The intrinsic damping of the molecules is included via $\sum_i \mathcal{L}_{\sigma_i}(\rho) = \sum_i \mathcal{L}_{S_i}(\rho)$. The transformation into the basis of the polariton states further changes the form of the incoherent damping of the cavity. In the secular approximation, the cavity damping Lindblad term, $\mathcal{L}_a(\rho)$, transforms as

$$\mathcal{L}_a(\rho) \approx \mathcal{L}_{S_+}(\rho) + \mathcal{L}_{S_-}(\rho), \tag{S10}$$

with respective decay rates

$$\gamma_{S_+} = \sin^2\theta\gamma_a, \tag{S11}$$
$$\gamma_{S_-} = \cos^2\theta\gamma_a. \tag{S12}$$

The contribution of the intrinsic molecular decay γ_σ to the decay of $|+\rangle$ and $|-\rangle$ can be neglected compared to the large cavity losses γ_a.

A. Elimination of the dephasing reservoir in the collective case

Here we derive the effective Lindblad terms that govern the incoherent processes induced by the interaction of the exciton-cavity-mode system with the dephasing reservoir, as discussed in the main text. For simplicity, we further assume that the intermolecular coupling is negligible and only weakly perturbs the dynamics given by Eq. (S9a) to Eq. (S9e). We eliminate the reservoir whose dynamics is given by the Hamiltonian term $H_\mathrm{res} = \sum_\alpha \hbar\Omega_\mathrm{R} B_\alpha^\dagger B_\alpha$ and the Lindblad terms $\sum_\alpha \mathcal{L}_{B_\alpha}(\rho)$, with $\gamma_{B_\alpha} = \gamma_B$ by standard methods of the theory of open-quantum systems using the secular approximation [1].

Eq. (S9b) represents the incoherent interaction between the upper, $|+\rangle$, and the lower, $|-\rangle$, polariton in close analogy with the single-excitonic case presented in the main text and leads to the Lindblad terms $\mathcal{L}_{S_\pm^\dagger S_\mp}(\rho)$ (i.e. the terms $\mathcal{L}_{S_+^\dagger S_-}(\rho)$ and $\mathcal{L}_{S_-^\dagger S_+}(\rho)$ using the compact notation). We further define $F_\alpha = d_\mathrm{R}\Omega_\mathrm{R}(B_\alpha + B_\alpha^\dagger)$ ($F_\alpha = F$ as the reservoir modes are equivalent) and note that

$$\langle F_\alpha^\dagger(t+s)F_\beta(t)\rangle = \delta_{\alpha\beta}\langle F_\alpha^\dagger(t+s)F_\alpha(t)\rangle = \delta_{\alpha\beta}\langle F^\dagger(t+s)F(t)\rangle \tag{S13}$$

as the respective bath modes are locally interacting with each molecule and are assumed to be uncorrelated. The respective rates then become

$$\gamma_{S_\mp^\dagger S_\pm} = \frac{\sin^2\theta\cos^2\theta}{N} J(\omega_\pm - \omega_\mp), \tag{S14}$$

which can be found from

$$\begin{aligned}
&\frac{\gamma_{S_\mp^\dagger S_\pm}}{\sin^2\theta\cos^2\theta} = \\
&= 2\Re\left\{\int_0^\infty \mathrm{d}s\, e^{i(\omega_\pm-\omega_\mp)s}\left\langle\sum_\alpha c_{\alpha1}c_{\alpha1}F_\alpha^\dagger(t+s)\sum_\beta c_{\beta1}c_{\beta1}F_\beta(t)\right\rangle\right\} \\
&= 2\Re\left\{\int_0^\infty \mathrm{d}s\, e^{i(\omega_\pm-\omega_\mp)s}\left\langle\sum_\alpha c_{\alpha1}^2c_{\alpha1}^2F_\alpha^\dagger(t+s)F_\alpha(t)\right\rangle\right\} \\
&= \sum_\alpha c_{\alpha1}^2c_{\alpha1}^2J(\omega_\pm-\omega_\mp) = \frac{1}{N}J(\omega_\pm-\omega_\mp), \qquad \text{(S15)}
\end{aligned}$$

where we have used the definition of the coefficients $c_{\alpha1} = 1/\sqrt{N}$ and

$$J(\omega) = 2\Re\left\{\int_0^\infty \mathrm{d}s\, e^{i\omega s}\langle F^\dagger(t+s)F(t)\rangle\right\} \qquad \text{(S16)}$$

to obtain the final result.

From Eq. (S9c) we obtain for the upper polariton the terms

$$\mathcal{L}_{\sum_{i=2}^N S_i^\dagger S_+}(\rho) \approx \sum_{i=2}^N \mathcal{L}_{S_i^\dagger S_+}(\rho), \qquad \text{(S17)}$$

$$\mathcal{L}_{\sum_{i=2}^N S_+^\dagger S_i}(\rho) \approx \sum_{i=2}^N \mathcal{L}_{S_+^\dagger S_i}(\rho), \qquad \text{(S18)}$$

where we neglected the Lindblad superators containing the cross-terms. In analogy with $\gamma_{S_\mp^\dagger S_\pm}$, the respective rates are

$$\gamma_{S_i^\dagger S_+} = \frac{\cos^2\theta}{N}J(\omega_+-\omega_0), \qquad \text{(S19)}$$

$$\gamma_{S_+^\dagger S_i} = \frac{\cos^2\theta}{N}J(\omega_0-\omega_+). \qquad \text{(S20)}$$

In close analogy, from Eq. (S9d) we get for the lower polariton

$$\mathcal{L}_{\sum_{i=2}^N S_i^\dagger S_-}(\rho) \approx \sum_{i=2}^N \mathcal{L}_{S_i^\dagger S_-}(\rho), \qquad \text{(S21)}$$

$$\mathcal{L}_{\sum_{i=2}^N S_-^\dagger S_i}(\rho) \approx \sum_{i=2}^N \mathcal{L}_{S_-^\dagger S_i}(\rho), \qquad \text{(S22)}$$

where we neglected the Lindblad superators containing the cross-terms. In analogy with $\gamma_{S_\mp^\dagger S_\pm}$, the respective rates are

$$\gamma_{S_i^\dagger S_-} = \frac{\sin^2\theta}{N}J(\omega_--\omega_0), \qquad \text{(S23)}$$

$$\gamma_{S_-^\dagger S_i} = \frac{\sin^2\theta}{N}J(\omega_0-\omega_-). \qquad \text{(S24)}$$

Last, we obtain the pure dephasing and energy transfer among the dark polariton states $\mathcal{L}_{\mathcal{S}}(\rho)$ ($\mathcal{S} = \cos^2\theta S_+^\dagger S_+ + \sin^2\theta S_-^\dagger S_- + \sum_{ij=2}^N S_i^\dagger S_j$). These terms do not contribute to the population decay and we will not consider them in the following.

B. Decay of the polariton states

The effective polariton dynamics derived above leads to the following rate equations (without the driving terms) of the polariton populations $n_+ = \langle S_+^\dagger S_+\rangle$, $n_\mathrm{D} = \frac{1}{N-1}\sum_{i=2}^N\langle S_i^\dagger S_i\rangle$ and $n_- = \langle S_-^\dagger S_-\rangle$

$$\begin{bmatrix}\dot{n}_+\\ \dot{n}_\mathrm{D}\\ \dot{n}_-\end{bmatrix} = \begin{bmatrix}-\gamma_{S_+}-\gamma_{S_-^\dagger S_+}-(N-1)\gamma_{S_\mathrm{D}^\dagger S_+} & (N-1)\gamma_{S_+^\dagger S_\mathrm{D}} & \gamma_{S_+^\dagger S_-}\\ \gamma_{S_\mathrm{D}^\dagger S_+} & -\gamma_{S_\mathrm{D}}-\gamma_{S_-^\dagger S_\mathrm{D}}-\gamma_{S_+^\dagger S_\mathrm{D}} & \gamma_{S_\mathrm{D}^\dagger S_-}\\ \gamma_{S_-^\dagger S_+} & (N-1)\gamma_{S_-^\dagger S_\mathrm{D}} & -\gamma_{S_-}-(N-1)\gamma_{S_\mathrm{D}^\dagger S_-}-\gamma_{S_+^\dagger S_-}\end{bmatrix}\begin{bmatrix}n_+\\ n_\mathrm{D}\\ n_-\end{bmatrix}, \qquad \text{(S25)}$$

where we used the equivalence of the dark-polariton states (neglecting the influence of the inter-molecular coupling) and defined $\gamma_{S_i^\dagger S_\xi} \equiv \gamma_{S_\mathrm{D}^\dagger S_\xi}$ and $\gamma_{S_\xi^\dagger S_i} \equiv \gamma_{S_\xi^\dagger S_\mathrm{D}}$ for $i > 1$ and the index $\xi \in \{+, -\}$.

The rate equations can be solved for a given initial condition. We present the results in the main text and compare them with the results of the full model.

2. HILBERT SPACE FOR THE NUMERICAL CALCULATIONS

In order to solve the dynamics given by the system Hamiltonian and the Lindblad terms as described in the main text, we need to define a suitable basis for the combined plasmonic, excitonic and vibrational Hamiltonian. We treat the plasmon and exciton on the same footing in the single-excitation manifold. We write the set of the cavity mode-exciton states as

$$\begin{aligned}
|\psi_{\mathrm{P-E}}\rangle =& s_0|0_\mathrm{p}, 0, 0, \ldots, 0\rangle \\
&+s_\mathrm{p}|1_\mathrm{p}, 0, 0, \ldots, 0\rangle \\
&+s_1|0_\mathrm{p}, 1, 0, \ldots, 0\rangle \\
&+s_2|0_\mathrm{p}, 0, 1, \ldots, 0\rangle + \ldots,
\end{aligned}$$

where the first occupation number represents the number of the cavity excitations and the following ones belong to the respective molecular excitons. Alternatively, the states $|1_\mathrm{p}, 0, 0, \ldots, 0\rangle$ and $|0_\mathrm{p}, 1, 0, \ldots, 0\rangle$ can represent the lower $|-\rangle$ and upper $|+\rangle$ polariton, respectively.

The reservoir states are represented in the double-excitation

basis as

$$\begin{aligned}|\psi_{\rm res}\rangle &= v_1|0,\,0,\,0,\ldots,\,0\rangle\\ &+ v_2|1,\,0,\,0,\ldots,\,0\rangle\\ &+ v_3|0,\,1,\,0,\ldots,\,0\rangle + \ldots\\ &+ w_1|2,\,0,\,0,\ldots,\,0\rangle\\ &+ w_2|1,\,1,\,0,\ldots,\,0\rangle\\ &+ w_3|1,\,0,\,1,\ldots,\,0\rangle + \ldots\\ &+ w_{N+1}|0,\,2,\,0,\ldots,\,0\rangle\\ &+ w_{N+2}|0,\,1,\,1,\ldots,\,0\rangle + \ldots\end{aligned}$$

The total state of the system is defined as a Kronecker product of the cavity mode-exiton and reservoir states

$$|\psi_{\rm tot}\rangle = |\psi_{\rm P-E}\rangle \otimes |\psi_{\rm res}\rangle.$$

This basis defines the dimension of the Hilbert space. With the number of molecules N the dimension of the Hilbert space $\mathcal{H}$ grows as $\mathrm{Dim}\,\{\mathcal{H}\} = \mathrm{Dim}\,\{|\psi_{\rm tot}\rangle\} = (N+1)(N+2)^2/2$. Moreover, the superoperator space necessary for the solution of the quantum master equation has the dimension $\mathrm{Dim}\{\mathcal{S}\} = \mathrm{Dim}\,\{\mathcal{H}\}^4$, which makes the numerical treatment of systems containing larger number of molecules difficult. In the main text we thus present results for up to $N = 5$ molecules.

3. CALCULATION OF THE INCOHERENT EMISSION SPECTRA AND THE ABSORPTION SPECTRA

The full model containing the incoherent dynamics presented in the main text can be solved numerically for smaller numbers of molecules. Here we discuss the technical details of the practical implementation of the calculation of the emission spectra.

The emission spectra of molecules can be calculated from the two-time correlation function as

$$s_{\rm E}(\omega;\omega_{\rm L}) = 2\Re\int_0^\infty \langle\langle a^\dagger(0)a(\tau)\rangle\rangle_{\rm ss}\, e^{{\rm i}\omega\tau}{\rm d}\,\tau \qquad \text{(S26)}$$

or equivalently

$$s_{\rm E}(\omega;\omega_{\rm L}) = 2\Re\int_0^\infty \langle\langle a^\dagger(\tau)a(0)\rangle\rangle_{\rm ss}\, e^{-i\omega\tau}{\rm d}\,\tau, \qquad \text{(S27)}$$

where we assume that the system is in the steady state induced by the pumping laser for $t = 0$ and $\langle\langle a^\dagger(\tau)a(0)\rangle\rangle_{\rm ss} = \langle a^\dagger(\tau)a(0)\rangle_{\rm ss} - \lim_{\tau\to\infty}\langle a^\dagger(\tau)a(0)\rangle_{\rm ss}$. On the other hand, the absorption spectra are obtained from

$$s_{\rm A}(\omega) = 2\Re\int_0^\infty \langle a(\tau)a^\dagger(0)\rangle_{\rm ss}\, e^{i\omega\tau}{\rm d}\,\tau \qquad \text{(S28)}$$

and we calculate the two-time correlation function with respect to the ground state of the system. We can apply the quantum regression theorem to obtain the effective dynamics of the two-time correlator.

We assume the equation of motion for the density matrix (the quantum master equation) in the form

$$\dot\rho = \mathcal{L}\rho, \qquad \text{(S29)}$$

with ρ represented by a column vector and $\mathcal{L}$ a superoperator matrix constructed from the Hamiltonian and Lindblad terms. The quantum regression theorem (QRT) then states

$$\langle O_1(t+\tau)O_2(t)\rangle = \mathrm{Tr}\left\{O_1(0)e^{\mathcal{L}\tau}\left[O_2(0)\rho(t)\right]\right\}. \qquad \text{(S30)}$$

In other words, the time evolution of the two-time correlator $\langle O_1(t+\tau)O_2(t)\rangle$ obeys the same dynamics as the mean-value of the Schrödinger-picture operator O_1, but with initial condition given by the operator $P = O_2(0)\rho(t)$ that replaces here the density matrix. More explicitly, the steady-state two-time correlation function reads in this notation (setting $t = 0$)

$$\langle O_1(\tau)O_2(0)\rangle = \mathrm{Tr}\left\{O_1(0)P(\tau)\right\}. \qquad \text{(S31)}$$

In the practical implementation we first calculate the initial value of P as $P(0) = O_2(0)\rho(0)$, where $\rho(0)$ is the steady-state density matrix fulfilling

$$\mathcal{L}\rho(0) = 0, \qquad \text{(S32)}$$

together with

$$\mathrm{Tr}\{\rho\} = 1. \qquad \text{(S33)}$$

The time evolution of P is obtained by integration of the equation

$$\dot P = \mathcal{L}P \qquad \text{(S34)}$$

using standard numerical methods. The spectrum is finally obtained by explicit calculation of the Fourier transform of the two-time correlation function as defined in Eq. (S27).

Last, we remark that the same method is applicable for calculation of the weak-probe absorption spectra given by simply exchanging the operators O_1 and O_2 and replacing $\omega \to -\omega$.

4. DEPENDENCE OF THE EMISSION AND ABSORPTION SPECTRA OF POLARITONS ON THE EFFECTIVE RESERVOIR FREQUENCY $\Omega_{\rm R}$ AND THE POLARITON SPLITTING

In the main text we describe the effective dephasing reservoir as a broad damped harmonic oscillator of energy $\hbar\Omega_{\rm R} = 400\,$meV, width $\hbar\gamma_B = 400\,$meV and coupling to the molecular electronic levels via $d_{\rm R} \approx 0.173$, yielding the reservoir spectral density

$$J(\omega) = \frac{2\gamma_B d_{\rm R}^2\Omega_{\rm R}^2}{(\Omega_{\rm R}-\omega)^2 + \gamma_B^2}. \qquad \text{(S35)}$$

Here we briefly discuss the influence of the frequency $\Omega_{\rm R}$ on the observed emission spectra. To that end we calculate the polariton emission and absorption spectra [Fig. S1 (a) and (b), respectively] for $N = 4$ molecules illuminated at the frequency of the upper polariton ($\hbar\omega_{\rm L} = 2.2\,$eV) for a constant broadening $\hbar\gamma_B = 400\,$meV and varying $\hbar\Omega_{\rm R} = 100\,$meV, 200 meV, 300 meV and 400 meV. We adjust $d_{\rm R}$ such that $J(0)$ remains unchanged for all cases. For clarity, all of the spectra in Fig. S1 are normalized to the maximal value and vertically displaced.

Figure S1 (a) shows that as $\Omega_{\rm R}$ is decreasing (from top to bottom), the emission spectra slightly change symmetry, making the emission from the upper polariton slightly more pronounced but preserving the qualitative picture. On the other hand, the absorption spectra remain practically identical for all $\Omega_{\rm R}$, as shown in Fig. S1 (b).

Next we study the dependence of the polariton emission and absorption on the polariton splitting $\omega_+ - \omega_- = 2\sqrt{N}g$. The spectra are calculated considering the parameters of the reservoir $\hbar\Omega_{\rm R} = 400\,$meV, $\hbar\gamma_{\rm R} = 400\,$meV and $d_{\rm R} \approx 0.173$ and values of $\hbar g$ ranging from $\hbar g = 100\,$meV to $\hbar g = 300\,$meV. In all cases we consider $N = 4$ molecules and tune the pumping laser frequency to the frequency of the upper polariton ($\omega_{\rm L} = \omega_0 + \sqrt{N}g$). The

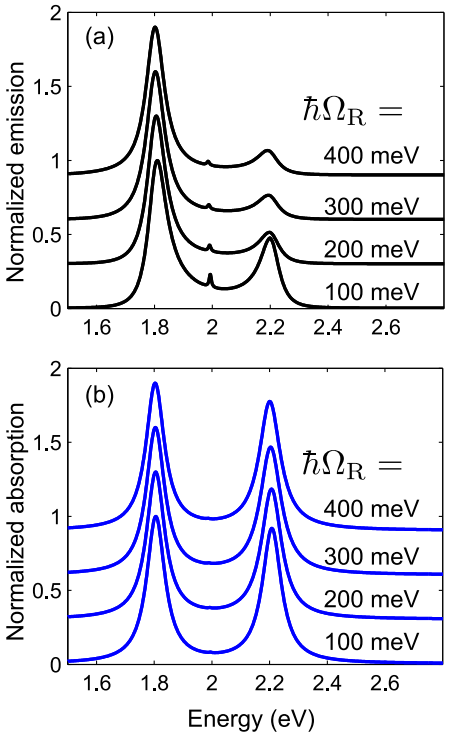

Fig. S1. Polariton (a) emission and (b) absorption spectra for $N = 4$ molecules illuminated at the frequency of the upper polariton ($\hbar\omega_L = 2.2\,\text{eV}$) for a constant broadening $\hbar\gamma_B = 400\,\text{meV}$ and varying $\hbar\Omega_R = 100\,\text{meV}$, 200 meV, 300 meV and 400 meV. We adjust d_R such that $J(0)$ remains unchanged for all cases. The spectra are calculated for $\hbar\omega_c = 2\,\text{eV}$, $\hbar g_i = \hbar g = 100\,\text{meV}$, $\hbar\mathcal{E} = 0.1\,\text{meV}$, $\hbar\gamma_a = 150\,\text{meV}$ and $\hbar\gamma_\sigma = 2\times10^{-2}\,\text{meV}$.

emission and absorption spectra are plotted in Fig. S2 (a) and (b), respectively. We normalize the spectra to the maximum of the lower-polariton peak and apply a constant vertical offset.

Increasing g leads to larger separation of the polariton spectral peaks in both the emission and the absorption spectra. In the emission spectra, the lower-polariton peak is more pronounced than the upper-polariton peak due to the asymmetric population transfer. Interestingly, the relative intensity of the upper-polariton peak with respect to the intensity of the lower-polariton peak is decreased when $2\sqrt{N}g \approx \Omega_R$, i.e. when the incoherent population transfer $|+\rangle \to |-\rangle$ becomes resonant [$J(\omega_+ - \omega_-)$ is maximized]. In the absorption spectra the upper- and lower-polariton peaks are of similar intensity.

REFERENCES

1. H.-P. Breuer and F. Petruccione, *The theory of open quantum systems* (Oxford University Press, 2003).

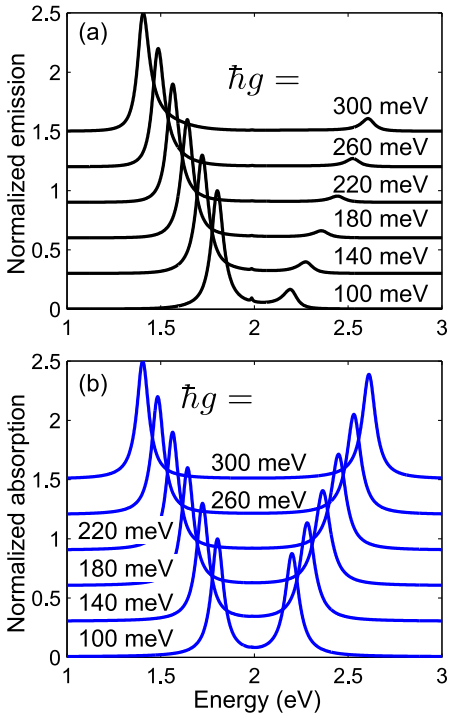

Fig. S2. Polariton (a) emission and (b) absorption spectra for $N = 4$ molecules illuminated at the frequency of the upper polariton for reservoir parameters $\hbar\gamma_B = 400\,\text{meV}$, $\hbar\Omega_R = 400\,\text{meV}$ and $d_R \approx 0.173$. The spectra are calculated for varying $\hbar g_i = \hbar g = 100\,\text{meV}$, 140 meV, 180 meV, 220 meV, 260 meV and 300 meV. The other model parameters are $\hbar\omega_c = 2\,\text{eV}$, $\hbar\mathcal{E} = 0.1\,\text{meV}$, $\hbar\gamma_a = 150\,\text{meV}$ and $\hbar\gamma_\sigma = 2\times10^{-2}\,\text{meV}$.